



# Error compensation in random vector double step saccades with and without global adaptation



Paul Zerr<sup>a,\*</sup>, Katharine N. Thakkar<sup>b</sup>, Siarhei Uzunbajakau<sup>a</sup>, Stefan Van der Stigchel<sup>a</sup>

<sup>a</sup> Helmholtz Institute, Department of Experimental Psychology, Utrecht University, The Netherlands

<sup>b</sup> Department of Psychology, Michigan State University, East Lansing, MI, USA

## ARTICLE INFO

### Article history:

Received 25 December 2015

Received in revised form 19 June 2016

Accepted 22 June 2016

Available online 2 September 2016

### Keywords:

Double step saccades

Spatial remapping

Saccade variability

Error compensation

Saccade adaptation

## ABSTRACT

In saccade sequences without visual feedback endpoint errors pose a problem for subsequent saccades. Accurate error compensation has previously been demonstrated in double step saccades (DSS) and is thought to rely on a copy of the saccade motor vector. However, these studies typically use fixed target vectors on each trial, calling into question the generalizability of the findings due to the high stimulus predictability.

We present a random walk DSS paradigm (random target vector amplitudes and directions) to provide a more complete, realistic and generalizable description of error compensation in saccade sequences. We regressed the vector between the endpoint of the second saccade and the endpoint of a hypothetical second saccade that does not take first saccade error into account on the ideal compensation vector. This provides a direct and complete estimation of error compensation in DSS. We observed error compensation with varying stimulus displays that was comparable to previous findings. We also employed this paradigm to extend experiments that showed accurate compensation for systematic undershoots after specific-vector saccade adaptation. Utilizing the random walk paradigm for saccade adaptation by Rolfs et al. (2010) together with our random walk DSS paradigm we now also demonstrate transfer of adaptation from reactive to memory guided saccades for global saccade adaptation.

We developed a new, generalizable DSS paradigm with unpredictable stimuli and successfully employed it to verify, replicate and extend previous findings, demonstrating that endpoint errors are compensated for saccades in all directions and variable amplitudes.

© 2016 Elsevier Ltd. All rights reserved.

## 1. Introduction

When observing the visual world we typically scan the environment with successive fast eye movements (saccades). This brings relevant objects onto the fovea, an area at the center of the retina specialized for color and sharp vision (e.g. Provis, Dubis, Maddess, & Carroll, 2013). For each of these saccades a motor vector is calculated based on current eye position and the saccade target, which requires gaze centered (retinotopic) spatial maps to be maintained and continuously revised. To update the representation of a retinotopic location after a saccade the visual system can rely either on visual input or, in its absence, on a positional recalculation based on spatial working memory and knowledge of eye displacement (remapping). Predictive remapping even before an eye movement is executed (Duhamel, Colby, & Goldberg, 1992) facilitates rapid programming of successive saccades. Predictive updating of

receptive fields has been observed in neuronal populations in the lateral intraparietal area (LIP) (e.g. Duhamel et al., 1992; Medendorp, Goltz, Vilis, & Crawford, 2003), superior colliculus (SC), extrastriate cortex, and frontal eye fields (FEF) (reviewed in Colby & Goldberg, 1999).

The double step saccade (DSS) task is commonly used to study spatial remapping in the absence of visual feedback (Hallett & Lightstone, 1976). In this paradigm two targets (**T1** and **T2**) are flashed briefly, and participants saccade from the fixation target (**F**) to **T1** (first saccade; **S1**) and from **T1** to **T2** (second saccade; **S2**). To successfully land on **T2**, its fovea-relative location after the saccade needs to be recalculated based on memory of its last known retinotopic position and the saccade vector to **T1**.

Errors in saccade landing positions create a mismatch between the ideal and actually executed motor vector. A motor vector is defined here as the actual saccadic motor output as measured by the eye tracker. An ideal saccade is defined as the vector between the endpoint of the last saccade and the position of the current saccade target. In order to correctly remap a future target, landing

\* Corresponding author at: Heidelberglaan 1, 3584 CS Utrecht, The Netherlands.  
E-mail address: [p.zerr@uu.nl](mailto:p.zerr@uu.nl) (P. Zerr).

errors of the current saccade need to be accounted for. It has been suggested that a copy of the saccade motor vector (corollary discharge; **CD**) supplies eye displacement information necessary for spatial remapping (e.g. Guthrie, Porter, & Sparks, 1983; Sommer & Wurtz, 2006). Collins, Rolfs, Deubel, and Cavanagh (2009) observed that CD would closely represent the actual saccade and thus incorporate trial-by-trial saccade error. Joiner, FitzGibbon, and Wurtz (2010) recently reported near perfect compensation in second saccades for endpoint errors in first saccades. They observed a strong correlation between first saccade error and compensatory component of the second saccade in the opposite direction, a finding that is best explained by the availability of a CD vector containing saccade errors to the visual system.

Further support for the reliance of remapping on CD comes from studies of saccadic adaptation. In the intra-saccadic back-step task originally developed by McLaughlin (1967), participants make saccades to targets that are displaced slightly towards the previous fixation target as soon as a saccade is detected. Due to saccadic suppression, subjects are normally unaware of target displacement and instead the visual system detects apparent systematic overshoots and gradually shortens saccades (for reviews of saccade adaptation see Herman, Blangero, Madelain, Khan, & Harwood, 2013; Hopp & Fuchs, 2004; Iwamoto & Kaku, 2010; Pélissier, Alahyane, Panouilleres, & Tilikete, 2010). Tanaka (2003) examined remapping in monkeys with a DSS task using horizontal-vertical saccade pairs while gradually inducing adaptation in first saccades. By regressing the compensatory (horizontal) component of second saccades on the horizontal endpoint error of first saccades, he found that the monkeys were able to compensate for gain changes in first saccades to correctly land on T2 (82% and 85% respectively for the two monkeys used in the study). He concluded that at least half of the signal corresponding to a CD vector must have come from sites downstream from the site of adaptation (and therefore included information about the change in saccade amplitude). However, because induction of adaptation and probing of compensation occurred gradually and simultaneously, natural trial-by-trial error and variations in gain induced by adaptation were treated equally while these errors could potentially be represented differently in the visual system. Collins (2010) examined error compensation in a similar way in humans by again regressing the (compensatory) horizontal component of second saccades on the horizontal amplitude errors of first saccades. In contrast to Tanaka, Collins observed saccades before and after inducing adaptation. Identical regression slopes were observed in adapted and unadapted saccades (corresponding to around 74% compensation on average in both cases), indicating that the visual system is indeed aware of and compensates for systematic changes in saccade amplitudes. Despite the difference in amount of compensation reported these studies agree that first saccade endpoint errors are mostly accounted for in subsequent saccades.

The vast majority of the remapping literature depends on stimuli with fixed and limited target positions (Fig. 2A), which simplify analysis but may be less indicative of natural behavior and could create experimental confounds if subjects memorize the small set of stimulus locations. If this were the case, the accurate error compensation observed in these studies could be explained by a spatiotopic long-term memory representation of target locations rather than a reliance on trial-by-trial information from CD. Zimmermann (2013) reported spatiotopic displacement of a saccade target following saccade adaptation, indicating the potential of long-term spatiotopic memory of target locations after repeated exposure to the same stimuli. The global saccadic adaptation paradigm by Rolfs, Knapen, and Cavanagh (2010) liberated experiments that examine the effect of adaptation on spatial remapping from this restriction. In their adaptation task targets appeared at random positions on the screen in each trial, and saccades were suc-

cessfully adapted for all directions (parametric adaptation). This provided a means for studying saccade adaptation as a global change in the saccade system. Our study aimed to extend previous studies that examined saccades in the DSS paradigm with and without adaptation by utilizing highly variable (and thus unpredictable) stimulus displays. In the first experiment we first introduce a novel DSS paradigm with random target vectors (Fig. 2B) and accompanying analysis method (Fig. 4) as well as models using simulating data to validate this method (Fig. 5). We then examined error compensation in a slow-paced (high pre-programming) and fast-paced (low pre-programming) DSS task. Ditterich, Eggert, and Straube (1998) suggested that high pre-programming should reduce error compensation in sequences because saccades are then executed based on fixed amplitudes. In this case better error compensation should be observed in our fast condition. In a second experiment we compared the amount of error compensation in second saccades before and after *global* saccade adaptation in the context of random target vectors. If, as has been suggested, CD contains adapted motor vectors then we should observe appropriate error compensation after adaptation.

It is so far unknown to what extent the mechanism for global adaptation differs from that of specific vector adaptation. Until recently the mechanism behind saccadic adaptation has been thought to be highly selective for the adapted saccade vector in terms of position, direction and amplitude as well as for saccade type (e.g. reactive versus memory guided). Transfer to other vectors was found to be very limited (Deubel, 1995; Noto, Watanabe, & Fuchs, 1999) and results for transfer to other saccade types has been mixed (for an overview see Pélissier et al., 2010; Kojima, Fuchs, & Soetedjo, 2015). The existence of context specific adaptation beyond specificity to particular vectors demonstrates that saccade adaptation is not just a simple motor recalibration process depending on motor states such as orbital eccentricity but can use predictive visual cues to change saccade metrics depending on visual properties of saccade targets (Azadi & Harwood, 2014). For instance, Herman, Harwood, and Wallman (2009) found specific adaptation to flickering versus non-flickering stimuli. However, these results have usually been obtained by adapting only one or a few specific vectors. Rolfs et al. (2010) demonstrated that global adaptation for all saccade directions and amplitudes is possible when displaying targets in a random walk design instead of using fixed vector positions. Importantly, they demonstrated that saccades were not simply adapted for many different vectors but that this adaptation was *parametric*: a global change in the saccade system. We examined for the first time whether this type of adaptation also transfers between saccade types. If transfer of global adaptation is limited to saccade type, we would expect that adaptation for the second (memory guided) saccades in the DSS task is reduced or absent as they are qualitatively different from the adapted (reactive) saccades. Conversely, if global adaptation is parametric beyond amplitude and direction both saccades should be adapted.

## 2. Material and methods

This study is approved by the Ethics Committee of the Faculty of Social and Behavioral Sciences of Utrecht University and has been carried out in accordance with The Code of Ethics of the World Medical Association (Declaration of Helsinki).

### 2.1. Participants

#### 2.1.1. Experiment 1

10 Utrecht University students (mean age:  $22.1 \pm 3.7$ ) participated in the experiment and were rewarded with EUR 6 per hour.

All participants had normal or corrected to normal visual acuity and gave informed consent.

2.1.2. Experiment 2

20 Utrecht University students (mean age: 23.6 ± 4.8) participated in the experiment and were rewarded with course credits or EUR 7 per hour. 10 participants were pseudo-randomly assigned to the adaptation group and 10 to the control group. All participants had normal or corrected to normal visual acuity and gave informed consent. Participants were debriefed about the adaptation procedure following completion of the experiment.

2.2. Materials

Stimuli were displayed on a 19" Nokia Multigraph 446Xpro CRT monitor with an effective display area of 36 × 27 cm, except for the first four participants in Experiment 2, for whom stimuli were displayed on a 21" Lacie Electron 22 Blue IV CRT monitor with an effective display area of 36 × 26 cm. Stimuli sizes and distances were computed to be identical on both monitors. Both monitors operated on a resolution of 1024 × 768 at a refresh rate of 120 Hz. To avoid visual referencing cues from CRT afterglow, a 4-stop neutral density filter was attached to the screen. Monocular eye movements were recorded by an Eyelink1000 eye tracker (SR Research Ltd, Canada) on a Windows machine at a temporal resolution of 1000 Hz and a spatial resolution of 0.01°. Participants were seated on an adjustable chair and placed their head on a chinrest. The screen was positioned 70 cm from the front edge of the chinrest. To prevent visual guidance the experiment took place in a room with near-absolute darkness with the exception of stimuli and the Eyelink1000 illuminator glow. The experiment was designed with PyGaze (Dalmajer, Mathôt, & Van der Stigchel, 2013), a python toolbox for eyetracking experiments based in this case on the Psychopy and Pylink python libraries.

2.3. Procedure

2.3.1. Experiment 1

Two conditions were tested in each experiment session, a slow-paced and a fast-paced double step saccade task. All sessions began with verbal and on-screen instructions, an eye tracker calibration and practice trials for each condition, followed by a number of calibration trials (see below) for the fast condition to determine how fast participants could initiate saccades. Afterwards participants

performed 4 blocks of 100 fast or slow trials each with breaks and eye tracker recalibration between blocks (Fig. 1). Sessions lasted about 85 min.

All trials began with a blue fixation target (F; empty circle, diameter = 0.5°) appearing at a random location within the effective display area. In slow trials, after participants pressed the space bar and fixation was detected for 250 ms, the fixation became a filled circle and after a random delay of 800–1500 ms a gray, filled target circle appeared. After 200 ms a second gray target circle appeared. 200–800 ms later the fixation dot disappeared, signaling participants to begin the saccade sequence. Target configurations are described in Fig. 2B below. As soon as gaze was detected 3° outside of fixation the targets disappeared, leaving a blank screen at the end of the first saccade. The location of the second target therefore had to be remapped based on memory and extra-retinal cues.

In the fast condition (low pre-programming) the fixation circle became filled after participants pressed the space bar and after 500 ms the second target appeared first on the screen. Then, after a delay of 300 ms the first target appeared and the fixation circle disappeared, signaling participants to initiate saccades. If the saccade to the first target was not detected within a threshold period (see calibration procedure below) the screen was blanked, a warning beep sounded and the trial was repeated. Since the first target appeared after the second target this greatly reduced the time the visual system had available to pre-program the second saccade (e.g. Li & Andersen, 2001). Previous to the experimental trials, during threshold calibration, fast trial types were repeated until ten consecutive trials were executed without repeat. If a trial was repeated three times in a row, the threshold value was increased by 100 ms, starting at 100 ms up to a maximum of 500 ms. Mean threshold was 360 ms ± 70 ms. During the experimental trials this served to force participants to begin programming the first saccade as soon as the first target appeared. During all trials, if gaze moved more than 2° from fixation before the go signal, the trial was terminated and repeated.

2.3.2. Experiment 2

Participants received verbal and on-screen instructions and practiced the task with 15 adaptation and 15 DSS trials. 100 DSS trials measured baseline gain and were followed by 100 adaptation trials with a 25% back-step and 100 adaptation trials with a 35% back-step. Subsequently 50 cycles of 4 adaptation plus 2 DSS trials produced 300 test trials (Fig. 3). Sessions lasted about 75 min. The interleaved adaptation trials ensured that saccades remained

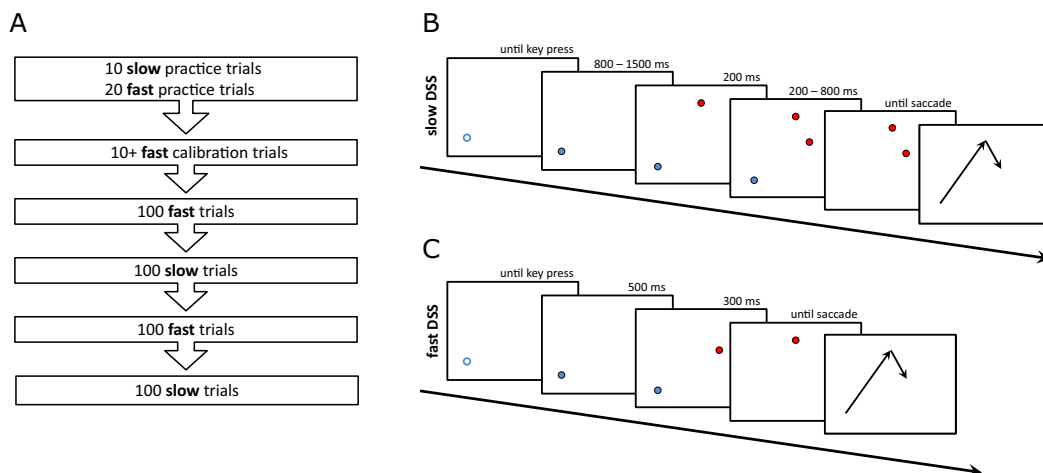
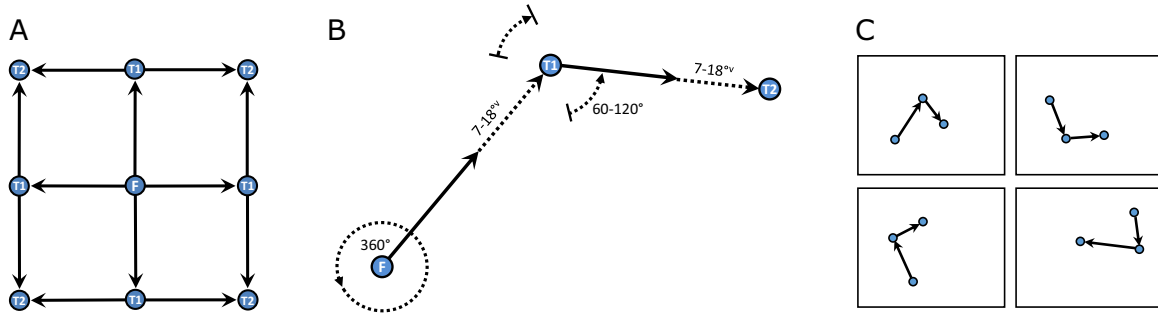
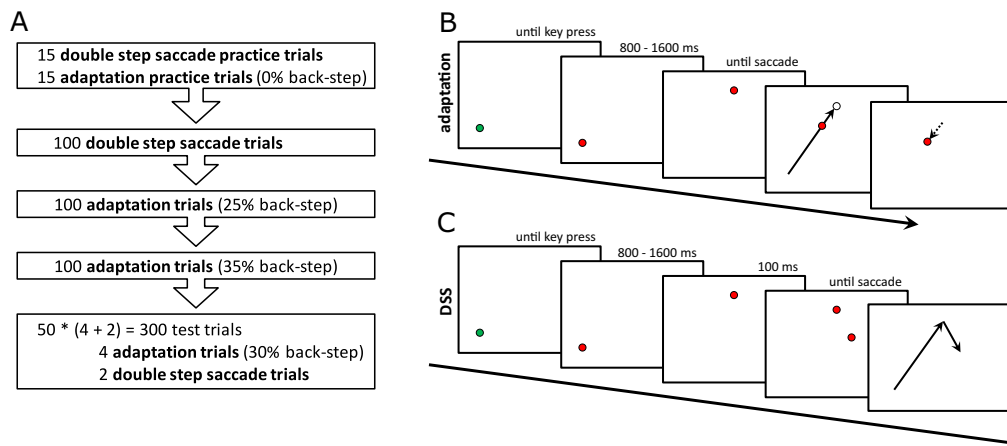


Fig. 1. (A) Experimental sequence Experiment 1. (B) Slow paced DSS task. Colors and background changed for visual clarity. Arrows indicate expected eye movement path. (C) Fast paced DSS task. (For interpretation of the references to colour in this figure legend, the reader is referred to the web version of this article.)



**Fig. 2.** (A) A typical array of possible stimulus configurations in previous DSS tasks. This creates only 4 possible endpoint locations. (B) Possible target configuration in the present study. Fixation (F) could appear anywhere on the effective display area. The first target (T1) could appear anywhere around F but at a distance of least  $7^\circ$  and a maximum of  $18^\circ$ . The second target (T2) could appear at a distance of  $7\text{--}18^\circ$  from T1, but with a polar angle between the first and second target vector of  $60\text{--}120^\circ$ .  $^\circ$  = polar angle;  $^\circ\text{v}$  = visual angle. (C) Four example trial configurations.



**Fig. 3.** (A) Experimental sequence Experiment 2. (B) Adaptation trials. Colors and background changed for visual clarity. Arrows indicate expected eye movement path. (C) DSS trials. (For interpretation of the references to colour in this figure legend, the reader is referred to the web version of this article.)

adapted throughout the session. Participants were allowed to take short breaks (black screen) while remaining seated after 100, 200, 300 and 450 test trials with one recalibration after the first break. To ensure that adaptation effects were not caused by fatigue or learning (Golla et al., 2008), a control group performed the experiment without target back-step in the adaptation task.

To ensure maximum transfer of adaptation, in this experiment the DSS and adaptation tasks were designed to be as similar as possible in terms of stimuli and timing. All trials began with a green fixation target (F; filled circle, diameter =  $0.5^\circ$ ) appearing at a random location within the effective display area. After participants pressed the space bar to start the trial F turned red and after a random delay of 800–1600 ms jumped to a new location. If gaze moved more than  $2^\circ$  from F after the dot had turned red, the trial was terminated and repeated.

During DSS trials a second target appeared after 100 ms, signaling participants to initiate a saccade sequence to the targets in order of their appearance. When gaze was detected  $3^\circ$  outside the previously displayed F the targets disappeared so that T2 had to be targeted from memory after the first saccade. After a delay of 3200 ms to allow for the execution of the saccades the next F appeared at the previous location of T2. Target configurations are described in Fig. 2.

During adaptation trials participants saccaded to the first target as soon as it appeared with F simultaneously disappearing. When gaze was detected  $3^\circ$  outside the previously displayed fixation saccades were considered in progress and the target was displaced (stepped back) towards F. After a delay of 2000 ms to allow for

the execution of the saccade the next fixation target appeared at the location of the displaced target.

#### 2.4. Data analysis

Saccade detection was performed offline by SR Research software. Eye movements were considered saccades for velocities over  $35^\circ/\text{s}$  or accelerations over  $9500^\circ/\text{s}^2$ . Further data analysis was performed in python. In each DSS trial a saccade to T1 (referred to here as S1) and a saccade to T2 (referred to here as S2) was defined from saccades with amplitude  $>4^\circ$ . S1 was selected as the first saccade in the trial that followed T1 onset, started within a  $2^\circ$  radius around F and ended within  $7^\circ$  of T1. S2 was selected as the first saccade occurred after S1 if that ended within  $7^\circ$  of T2. An S1 made to T2 would lead to an S2 being made to T1, which would also invalidate the trial. If no two saccades in a trial satisfied these conditions, it was classified as invalid. These exclusion criteria resulted in a total loss of 13% of trials in Experiment 1 and 19% in Experiment 2. More conservative thresholds did not change the pattern of results reported but further reduced the dataset. The high proportion of invalid trials can be attributed to the difficulty of the task, in which stimulus locations were not predictable between trials. A subset of saccade configurations (around 10% of trials from different participants and conditions) were optically verified to ensure the validity of the saccade selection method. 10 participants in Experiment 1 were replaced because more than 40% of their trials were invalid to ensure that unmotivated or unable participants did not confound the results. To avoid selection bias the analyses were

repeated with all participants. This did not significantly alter the results.

Error compensation was computed as follows (also see Fig. 4): first saccade error can be described as a vector between the endpoint of the first saccade (E1) and T1. If the visual system does not take this error into account but assumes to have landed on T1, it will program the second saccade as the vector between T1 and T2. If this vector is executed from the actual gaze position E1, the endpoint of the second saccade will be placed at E2'. Thus, the vector required for full compensation ( $e_1$ ; the difference between E2' and T2) is identical to the first saccade error vector ( $error_1$ ). This vector can be broken down into a projection onto the line between F and T1 to produce a measure of ideal compensation in the direction of the first target vector ( $e_{1y}$ ) and a perpendicular component ( $e_{1x}$ ) to describe ideal compensation perpendicular to the first target vector. The same projections can be made for the vector from E2' to the second saccade endpoint E2 ( $e_2$ ) to produce the actual amount of compensation in direction of the first target vector ( $e_{2y}$ ) and perpendicular to it ( $e_{2x}$ ). The regression slopes between  $e_{2y}$  and  $e_{1y}$  and between  $e_{2x}$  and  $e_{1x}$  reflect the average amount of error compensation in these two directions. The y components describe compensation in second saccades for error in direction of the first target vector in first saccades (referred to here as amplitude error compensation). The x components describe compensation for error perpendicular to the direction of the first target vector in first saccades (referred to here as angular error compensation). A model for full compensation (where  $e_2$  is identical to  $e_1$  on every trial) is a perfect correlation between  $e_1$  and  $e_2$  if the second saccade does not introduce additional, unrelated error. Since there is always variance in saccades a true model for perfect compensation is the perfect correlation just described with variance added to  $e_2$  (Fig. 5A). A model describing no compensation is a fully independent  $e_1$  and  $e_2$  (Fig. 5B). This provides a very direct and complete measure of error compensation in DSS as the entire error vector

is taken into account. It is also unbiased by specific target vector amplitudes and angles. Linear regression was computed using the least-squares method, wherein slopes were optimized to minimize residuals in the vertical axis to give an estimate of the average compensation for endpoint error in the first saccade while disregarding unrelated variance of the second saccade. Average slopes between conditions were compared using paired-samples two-tailed *t*-tests. S1 latencies were defined as the start of the first saccade minus offset of the fixation dot in the slow DSS condition and as the start of the first saccade minus onset of T1. Intersaccadic intervals were defined as start of the second saccade minus end of the first saccade in both conditions.

In Experiment 2 saccade gain ( $S1_{GAIN}$  and  $S2_{GAIN}$ ) was defined as the ratio between saccade amplitude and the distance between saccade starting point and target. Gain change after adaptation was analyzed by a 2-way MANOVA.

### 3. Results

#### 3.1. Experiment 1

We investigated how saccades in a sequence correct for endpoint error of the previous saccade in a double step saccade task with random target vectors. To verify that the vector based analysis method is appropriate we produced two models using simulated data, one for no compensation (Fig. 5A) and one for full compensation (Fig. 5B). The no-compensation model was produced by regressing two independent random normal distributions, representing an uncorrelated  $e_1$  and  $e_2$ . Its regression slope is  $\sim 0$ , indicating  $\sim 0\%$  compensation. The full-compensation model was produced by plotting a random normal distribution ( $e_1$ ) against itself ( $e_2 = e_1$ ) with a random value from a separate random normal distribution added to the vertical coordinate of every point, representing an  $e_2$  that perfectly follows  $e_1$  (full compensation) but also introduces additional, non-systematic error. Its regression slope is

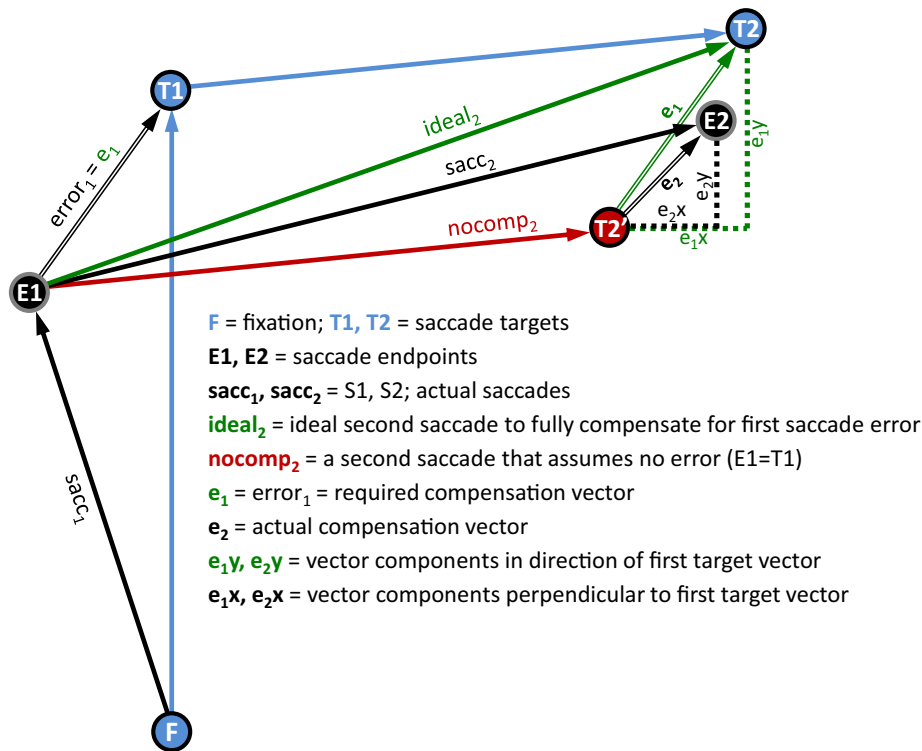
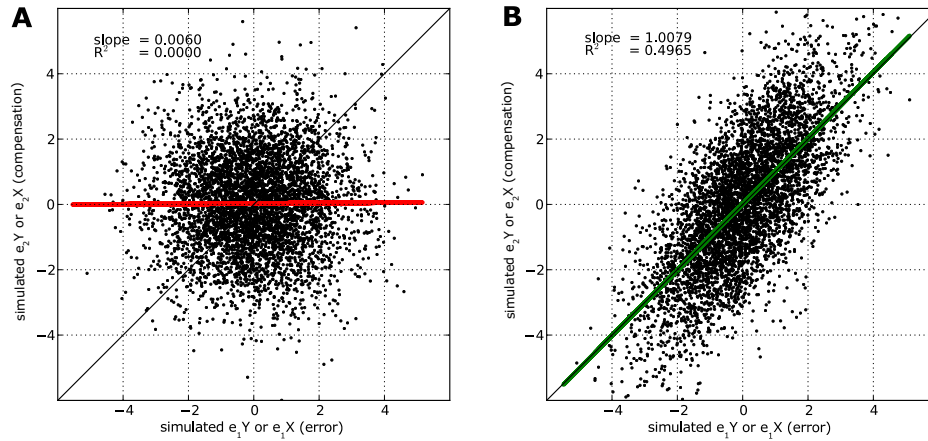
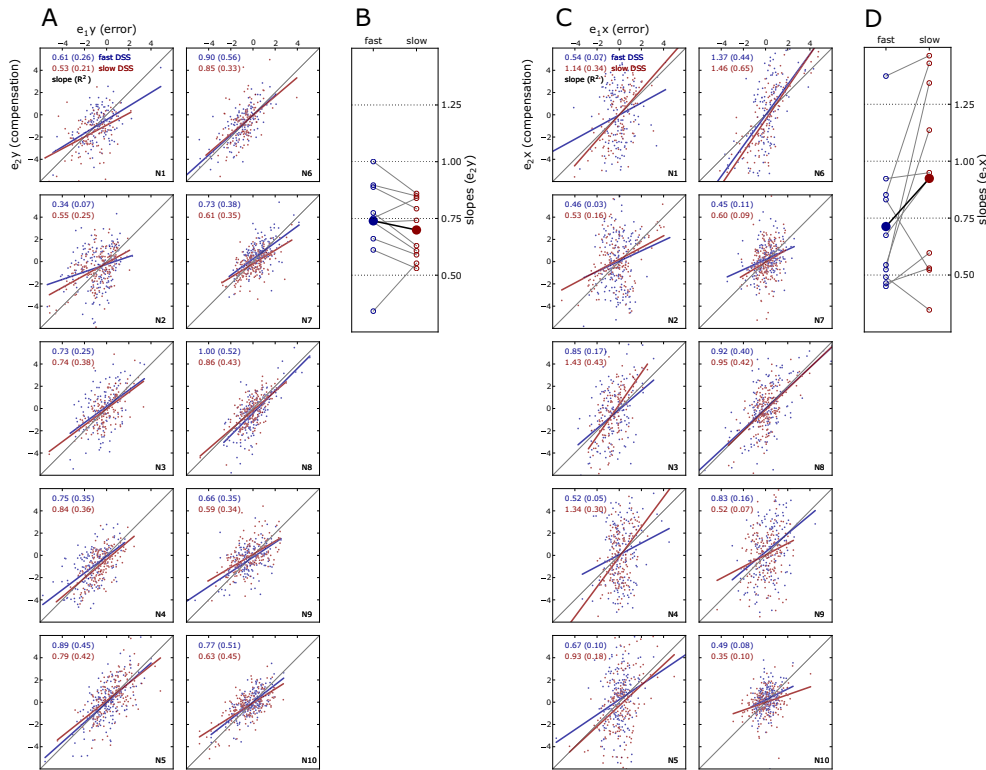


Fig. 4. Geometric representation of the analysis method on an example trial.



**Fig. 5.** Simulated data from normal distributions with variance parameters of the observed data. (A) Model for no compensation (independent  $e_1$  and  $e_2$ ). (B) Model for full compensation ( $e_2$  equals  $e_1$  on average). Units are visual degrees.



**Fig. 6.** Individual regression slopes indicating average error compensation. The diagonal line represents full compensation. Units are visual degrees. (A) Amplitude error compensation data per participant (for y projections). (B) Replotted error compensation slopes (for y projections). Empty circles represent slopes of individual participants, filled circles represent group means. (C) Angular error compensation per participant (for x projections). (D) Replotted error compensation slopes (for x projections). (For interpretation of the references to colour in this figure legend, the reader is referred to the web version of this article.)

$\sim 1$ , indicating  $\sim 100\%$  compensation. Note that without additional (unrelated) error in the second saccade all points would lie exactly on the red and green line. In a case of perfect compensation every deviation of  $e_1$  from 0 would be followed by an identical change in  $e_2$ . Conversely, with no compensation and otherwise perfect S2  $e_2$  would always be 0. Since all saccades introduce error, we included random and vertical spread. The regression lines optimize vertical variance and indicate the average amount of compensation for error in S1.

In the fast DSS condition the first target appeared after the second target and saccades had to be initiated quickly after its onset. This would reduce the time the visual system had available to pre-

program the second saccade along with the first saccade. The average regression slope from data of the ten participants was  $0.74 \pm 0.17$  (mean  $R^2 = 0.37 \pm 0.14$ ) for amplitude error compensation, indicating  $\sim 74\%$  compensation (blue lines in Fig. 6A). Average slope for compensation of angular error (approximating angular error) was  $0.71 \pm 0.28$  (mean  $R^2 = 0.16 \pm 0.14$ ), indicating 71% compensation (blue lines in Fig. 6C). In the slow DSS condition participants were not forced to saccade quickly and thus could more efficiently pre-program both saccades from the retinal vector. In this condition the average regression slope was  $0.70 \pm 0.12$  (mean  $R^2 = 0.35 \pm 0.07$ ) for amplitude error compensation, indicating  $\sim 70\%$  compensation (red lines in Fig. 6A). Average slope for angular

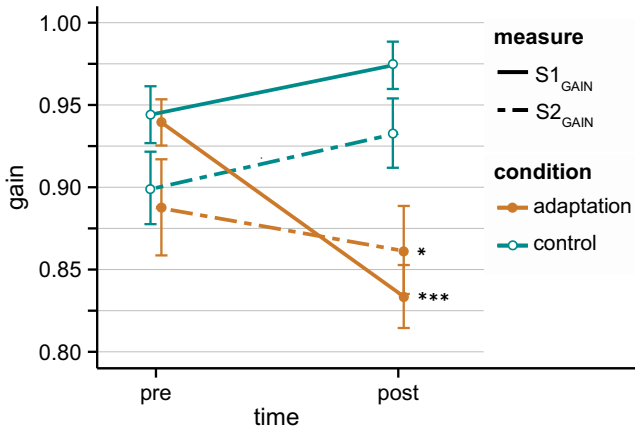


**Fig. 7.** Means of participant means before and after adaptation in both groups. Bars represent standard error.  $S1_{GAIN}$  and  $S2_{GAIN}$  decreased in the adaptation group but not in the control group. \* = sign. at 0.05 level. \*\*\* = sign. at 0.0001 level.

error compensation was  $0.92 \pm 0.39$  (mean  $R^2 = 0.27 \pm 0.18$ ), indicating 92% compensation (red lines in Fig. 6C). These data verify that saccade programming incorporates endpoint error of the previous saccade on a trial by trial basis, even when target vectors are randomly chosen for each trial.

Although there was a trend towards better compensation in the fast condition as seven out of ten participants showed this effect in amplitude error compensation (Fig. 6A and B) a paired-samples t-test revealed no significant evidence for a difference in compen-

sation slopes between conditions for compensation of amplitude ( $t(9) = 1.12, p = 0.29$ ) or angular error ( $t(9) = -1.89, p = 0.09$ ).

### 3.2. Experiment 2

To understand whether systematic saccade amplitude errors are also taken into account in the programming of subsequent saccades we compared error compensation in DSS before and after global saccade adaptation.

#### 3.2.1. Global saccade adaptation

We first examined the influence of the adaptation manipulation by comparing difference scores (change after adaptation) of  $S1_{GAIN}$  and  $S2_{GAIN}$ . A MANOVA identified significant gain changes on the group level (Wilks' Lambda = 0.266,  $F(1,18) = 23.48, p < 0.001, \eta^2 = 0.734$ ) in  $\Delta S1_{GAIN}$  ( $F(1,18) = 42.56, p < 0.0001, \eta^2 = 0.703$ ) and  $\Delta S2_{GAIN}$  ( $F(1,18) = 4.626, p = 0.045, \eta^2 = 0.204$ ). In other words, the gain change after adaptation differed significantly between adaptation and control group. The global adaptation procedure was successful and  $S1_{GAIN}$  (0.106 or 11.3% from baseline) and  $S2_{GAIN}$  (0.026 or 3.3% from baseline) in the DSS task were significantly reduced after the adaptation manipulation, but not in the control group.  $S1_{GAIN}$  and  $S2_{GAIN}$  tend to increase in the control group, which can be considered a learning effect whereby participants increase gain with practice. Adaptation is assumed to be working against this learning effect. This suggests that adaptation indeed transferred to S2. Fig. 7 illustrates gain results as means of participant means before and after adaptation for both groups. Fig. 8A and B visualize gains before and after adaptation as a func-

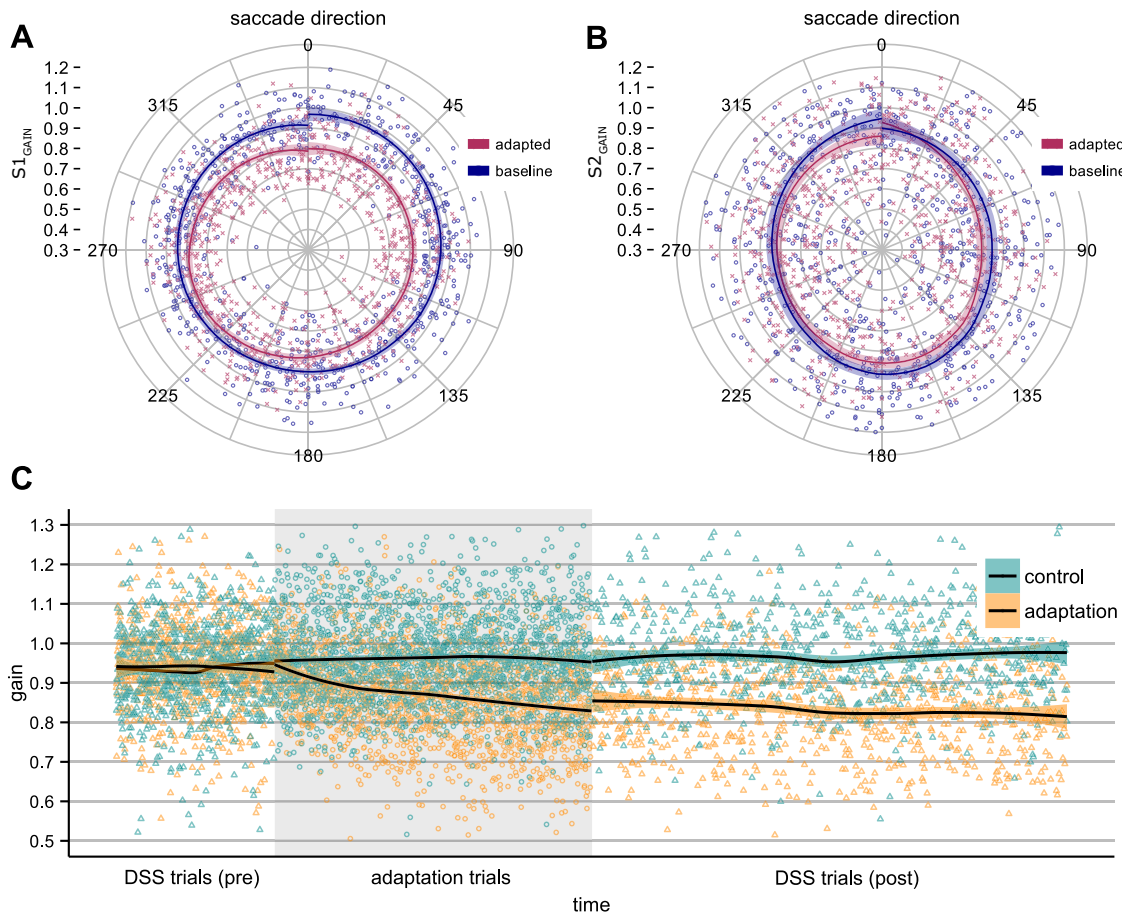


**Fig. 8.** Gain as a function of saccade direction in the adaptation group before and after adaptation for (A)  $S1$  and (B)  $S2$  in a Local Polynomial Regression (LOESS) fit ( $\alpha = 0.5$ ), folded into polar plots. Colored shadings represent 95% confidence intervals. (C) Adaptation timeline. “DSS trials (post)” displays values for  $S1_{GAIN}$  with the interleaved adaptation trials removed. Lines are LOESS fits ( $\alpha = 0.8$ ). Colored areas represent 95% confidence intervals.

tion of saccade direction. A timeline of adaptation is depicted in Fig. 8C. Amplitudes of saccades gradually reduced during adaptation trials and remained reduced throughout the post adaptation DSS trials. S1 latencies as measured from T1 onset (pre-adaptation: 318 ms + 120 ms, post-adaptation: 300 ms + 116 ms) confirmed that both targets were visible before S1 onset. These data demonstrate global saccadic adaptation for the trained saccade type (reactive) and suggests a moderate amount of transfer to memory guided saccades.

### 3.2.2. Error compensation in adapted DSS

Average regression slopes representing compensation for amplitude errors were not significantly different before (mean slope =  $0.58 \pm 0.38$ , mean  $R^2 = 0.19 \pm 0.17$ ) and after (mean slope =  $0.60 \pm 0.15$ , mean  $R^2 = 0.20 \pm 0.10$ ) adaptation (Fig. 9) in the adaptation group. Paired-samples two-tailed  $t$ -test:  $t(9) = -0.108$ ,  $p = 0.917$ . However, as can be seen in participant 4 (Fig. 9A) an identical regression slope does not mean that the adapted vector is taken into account. After adaptation mean error ( $e_1y$ ) was shifted to the left but mean compensation ( $e_2y$ ) did not shift downwards as would be expected if S2 were informed about the global reduction in S1 amplitudes. While in this participant compensation for S1 adaptation was not observed, Fig. 9B illustrates that most participants do take the adapted vector into account: an increase in error (shift to the left) is followed by an increase in compensation (shift downwards). Both the increase in error ( $t(9) = 6.04$ ,  $p = 0.0002$ ) and the corresponding change in the compensation vector ( $t(9) = 3.36$ ,  $p = 0.008$ ) were significant in repeated measures  $t$ -tests. This provides further evidence that during spatial remapping, extra-retinal signals from locations

downstream of the site of adaptation that contain the adapted vectors enable the visual system to take this change in saccade metrics into account.

## 4. Discussion

In this study we investigated saccade programming in a sequence without visual guidance after the onset of the first saccade and the degree to which natural and induced saccade endpoint error is compensated in a subsequent saccade. Any eye movement displaces retinotopic target coordinates and requires the target vector to be recomputed using an extra-retinal signal of eye displacement and the memorized pre-saccadic target vector. Saccade error disallows full reliance on pre-programmed (predicted) post-saccadic target vectors and has to be taken into account to correctly saccade to the next target location. Regressing the difference between a hypothetical second saccade that ignores previous endpoint error and the actual saccade on the vector required for full error compensation produced a percentual estimate of the average error compensation per condition and participant.

We developed a double step saccade paradigm that displays targets at random locations to exclude saccade targeting based on long-term memory of the spatial layout of the stimuli. Previous studies investigating double step saccades used fixed target configurations (Fig. 2A) that could easily have been memorized and saccades may have been corrected based on this memory instead of relying on CD. Joiner et al. (2010) reported very high error compensation for saccade pairs with identical amplitudes and a  $90^\circ$  angle separation between them. Angles of second sac-

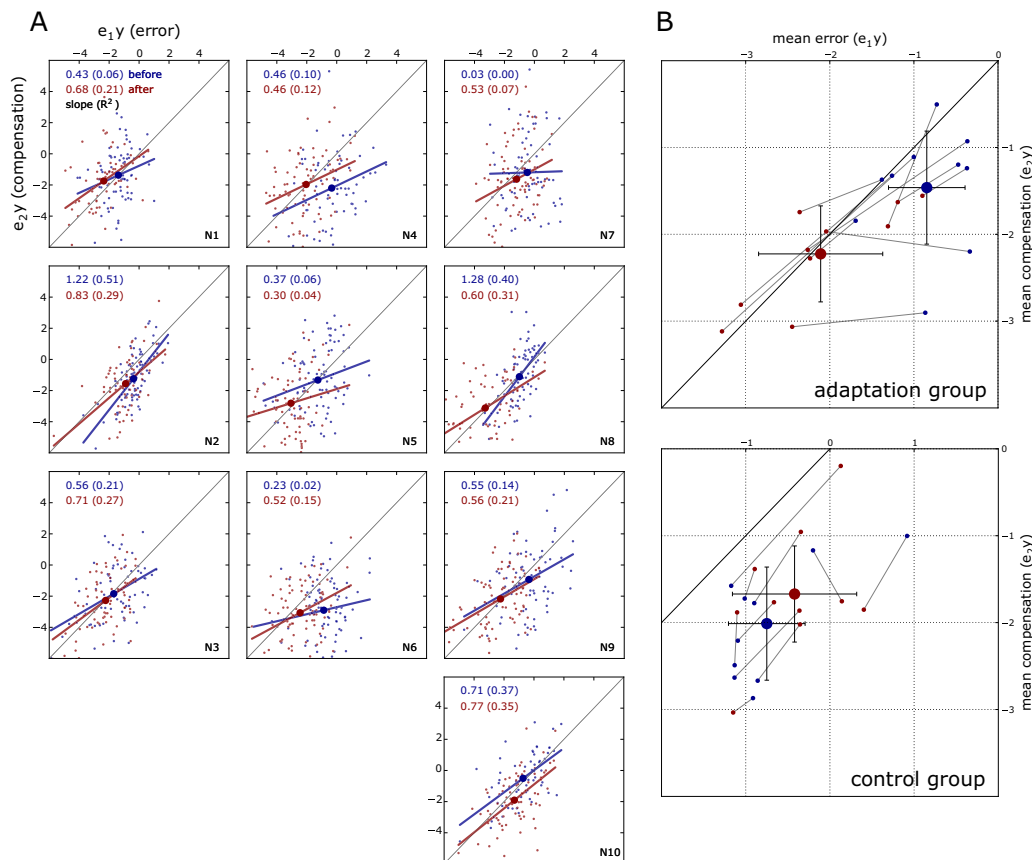


**Fig. 9.** (A) Individual regression slopes before and after adaptation in the adaptation group. (B) Mean values for error and compensation vectors. Large circles indicate mean of means. Error bars represent one standard deviation.



**Table 1**  
Median first saccade latencies and intersaccadic intervals in Experiment 1.

ppt	Slow DSS			Fast DSS		
	S1 latency	ISI	r (p)	S1 latency	ISI	r (p)
1	343	224	0.02 (0.82)	303	173	-0.05 (0.57)
2	308	296	0.03 (0.66)	359	321	-0.22 (0.00)
3	266	322	0.22 (0.01)	252	242	-0.01 (0.89)
4	240	310	0.01 (0.95)	284	209	-0.05 (0.51)
5	284	261	0.07 (0.36)	273	256	-0.04 (0.59)
6	356	261	-0.12 (0.16)	403	198	-0.12 (0.20)
7	775	329	-0.16 (0.03)	298	222	-0.18 (0.01)
8	274	248	0.27 (0.00)	275	221	-0.10 (0.17)
9	319	245	0.05 (0.57)	264	273	0.11 (0.14)
10	423	323	0.13 (0.06)	420	228	-0.13 (0.09)

ades compensated around 100% of amplitude error in horizontal-vertical saccade pairs, 74% in vertical-horizontal pairs and 90% in oblique saccades. Collins (2010) used a similar spatial target layout and reported 74% compensation on average. In the first experiment of the present study we found comparable results of 74% amplitude error compensation in fast DSS and 70% in slow DSS, demonstrating that endpoint error correction in DSS sequences is not dependent on long-term spatiotopic memory of target configurations alone. These results provide further evidence for the existence of a CD signal and the reliance of the saccade system on this signal.

We aimed to induce a high degree of pre-programming by presenting the second target after the first, without limiting the time available to initiate the first saccade, in order to allow the visual system to plan both saccade vectors before the initiation of the first saccade. This condition was most comparable to traditional DSS paradigms with the exception that the two targets are typically presented sequentially. Here their presentation time was partially overlapping to further increase pre-programming of the second saccade by providing clear visual vectors. In the fast DSS condition the second target was presented first and saccades had to be initiated immediately after the onset of the first target. A greater amount of compensation (steeper regression slopes) in this condition could have indicated that the visual system is aware of the decreased reliability of the pre-programmed second saccade and prioritizes information from a CD vector. However, differences in compensation between conditions were not significant. A limitation to these results is that the actual extent of pre-programming in the present DSS tasks cannot easily be quantified. A negative correlation between S1 latencies and ISI's has been suggested by Becker and Jürgens (1979) to indicate the extent of parallel processing prior to the onset of the first saccade. If participants had more time to pre-program both saccade vectors before initiating S1 then less time would be required to re-process S2 between saccades. For two reasons it is questionable whether this analysis can be applied to our results in Experiment 1. First, pre-programming would be expected in slow DSS. However, in this condition both targets were visible for a long time (200–800 ms random fixation offset delay plus S1 latency). It can be assumed that any parallel processing of the two saccades would have been concluded prior to S1 onset and would therefore not affect ISI's. Second, Becker & Jürgens instructed participants to follow the target as soon as it jumped, causing saccades with longer reaction times to be targeted to the second target jump location directly. In contrast, we specifically instructed participants to saccade to the first and then to the second target. S1 latencies, intersaccadic intervals and their correlation within subjects are described in Table 1. While the correlations are negative for nine of the ten subjects they are statistically significant in only 2. Further, paired-sample t-tests suggest that there was no difference in S1 latencies ( $t(9) = 0.93$ ,  $p = 0.38$ ). ISI's were even shorter in the fast condition ( $t(9) = 2.97$ ,

$p = 0.016$ ), although this could reflect the overall faster pace in this condition.

Future studies could investigate the precise relationship between parallel saccade processing and compensation by employing a continuous measure of pre-programming to address the question of how inputs from 'desired' and 'actual' saccade vectors are weighted to estimate eye displacement in the absence of visual feedback.

It is important to acknowledge the large variability between participants. For amplitude error compensation regression slopes ranged from 0.34 to 1.0. Variability in angle error compensation was even larger with slopes ranging from 0.34 to 1.42 in the slow DSS condition. In comparison, slopes ranged from 0.58 to 1.17 in the five participants in the study by Joiner et al. (2010). It is therefore not possible to converge on a global estimate of the amount of error compensation in the saccade system as this is highly variant from individual to individual. There appears to be within-subject consistency, however, as can be observed in the high correlation between compensation in the fast and slow DSS conditions of the present study, at least in amplitude error compensation (Pearson's  $r = 0.784$ ,  $p = 0.007$ ).

In Experiment 2 we investigated whether endpoint error caused by a systematic reduction of saccade amplitudes by adaptation is taken into account during error compensation. This is informative about possible neurophysiological sources of CD. If CD contains adapted vectors then saccade sequences should be executed correctly after adaptation. This is indeed what we found, in line with previous studies that reported veridical error compensation after adaptation of specific target vectors (e.g. Collins, 2010; Tanaka, 2003). Extra-retinal signals carrying adapted vectors must come from locations downstream from the site of adaptation. Converging evidence from lesioning studies (Barash et al., 1999; Goldberg, Musil, Fitzgibbon, Smith, & Olson, 1993; Takagi, Zee, & Tamargo, 1998), spike recordings (Catz, Dicke, & Thier, 2005, 2008; Soetedjo & Fuchs, 2006) and neuroimaging (Desmurget et al., 1998, 2000) strongly points to the cerebellum as the most likely site of adaptation. The superior colliculus has been suggested to relay CD signals via the thalamus to frontal eye fields (Sommer & Wurtz, 2004) but lies upstream from the cerebellum, making it an unlikely source of extra-retinal signals containing adapted vectors. One study found adaptation related activation in the SC (Takeichi, Kaneko, & Fuchs, 2007), contradicting reports by Frens and Van Opstal (1997). A more recent paper by Quessy, Quinet, and Freedman (2010) disagrees with the results by Takeichi et al. on methodological grounds and presents further evidence that amplitude encoding in SC is not altered by adaptation. Adaptation can transfer to saccades elicited by electric stimulation of the SC (Edelman & Goldberg, 2002; Fitzgibbon & Goldberg, 1986), further supporting the hypothesis that adaptation takes place downstream from the SC. Multiple pathways may contribute extra-retinal

signals as lesioning the SC-MD-FEF pathway has only partially disrupted spatial remapping (Sommer & Wurtz, 2002, 2006). Indeed, several subcortical structures downstream from the site of adaptation in the cerebellum send ascending projections to the thalamus (for an overview see Tanaka, 2003). Our results contribute to the hypothesis that at least one source of extra-retinal signals lies at or downstream from the cerebellum.

Studies investigating transfer of adaptation from reactive to memory guided saccade types have shown mixed results. Deubel (1995, 1999) found no evidence of transfer whereas other studies such as Hopp and Fuchs (2002, 2010), Fujita, Amagai, Minakawa, and Aoki (2002) and Panouillères et al. (2012) reported adaptation transfer of 50–100% from reactive to memory guided saccades. In our study S1 were reactive saccades (made to a visible target at onset) while S2 were memory guided. In line with the latter studies we observed a moderate but significant gain reduction in S2 after the adaptation procedure as compared to the control group. This suggests that with global (parametric) adaptation transfer from reactive to memory guided saccade types may also be occurring.

In summary, we present, test and apply a novel, random-walk based DSS paradigm capable of examining saccades of all directions and amplitudes and suggest that endpoint error compensation in saccade sequences relies on trial-by-trial CD even for random target configurations.

## Acknowledgments

We would like to thank Ignace Hooge for helpful discussions.

This research was funded by a VIDI Grant 45213008 from the Netherlands Organization for Scientific research to Stefan Van der Stigchel.

## References

- Azadi, R., & Harwood, M. R. (2014). Visual cues that are effective for contextual saccade adaptation. *Journal of Neurophysiology*, *111*(11), 2307–2319.
- Barash, S., Melikyan, A., Sivakov, A., Zhang, M., Glickstein, M., & Theier, P. (1999). Saccadic dysmetria and adaptation after lesions of the cerebellar cortex. *Journal of Neuroscience*, *19*, 10931–10939.
- Becker, W., & Jürgens, R. (1979). An analysis of the saccadic system by means of double step stimuli. *Vision Research*, *19*(9), 967–983.
- Catz, N., Dicke, P. W., & Thier, P. (2005). Cerebellar complex spike firing is suitable to induce as well as to stabilize motor learning. *Current Biology*, *15*, 2179–2189.
- Catz, N., Dicke, P. W., & Thier, P. (2008). Cerebellar-dependent motor learning is based on pruning a Purkinje cell population response. *Proc. Natl. Acad. Sci. U.S.A.*, *105*, 7309–7314.
- Colby, C. L., & Goldberg, M. E. (1999). Space and attention in parietal cortex. *Annual Review of Neuroscience*, *22*(1), 319–349. <http://dx.doi.org/10.1146/annurev.neuro.22.1.319>.
- Collins, T. (2010). Extraretinal signal metrics in multiple-saccade sequences. *Journal of Vision*, *10*(14), 7. <http://dx.doi.org/10.1167/10.14.7>.
- Collins, T., Rolfs, M., Deubel, H., & Cavanagh, P. (2009). Post-saccadic location judgments reveal remapping of saccade targets to non-foveal locations. *Journal of Vision*, *9*(5), 29.
- Dalmajier, E. S., Mathôt, S., & Van der Stigchel, S. (2013). PyGaze: An open-source, cross-platform toolbox for minimal-effort programming of eyetracking experiments. *Behavior Research Methods*, *1*–9. <http://dx.doi.org/10.3758/s13428-013-0422-2>.
- Desmurget, M., Pélisson, D., Grethe, J. S., Alexander, G. E., Urquizar, C., Prablanc, C., & Grafton, S. T. (2000). Functional adaptation of reactive saccades in humans: a PET study. *Experimental Brain Research*, *132*, 243–259.
- Desmurget, M., Pélisson, D., Urquizar, C., Prablanc, C., Alexander, G. E., & Grafton, S. T. (1998). Functional anatomy of saccadic adaptation in humans. *Nature Neuroscience*, *1*, 524–528.
- Deubel, H. (1995). Separate adaptive mechanisms for the control of reactive and volitional saccadic eye movements. *Vision Research*, *35*(23), 3529–3540. [http://dx.doi.org/10.1016/0042-6989\(95\)00058-M](http://dx.doi.org/10.1016/0042-6989(95)00058-M).
- Deubel, H. (1999). Separate mechanisms for the adaptive control of reactive, volitional, and memory-guided saccadic eye movements. In *Attention and performance XVII: Cognitive regulation of performance*.
- Ditterich, J., Eggert, T., & Straube, A. (1998). Fixation errors and timing in sequences of memory-guided saccades. *Behavioural Brain Research*, *95*(2), 205–217. [http://dx.doi.org/10.1016/S0166-4328\(97\)00160-5](http://dx.doi.org/10.1016/S0166-4328(97)00160-5).
- Duhamel Colby, C. L., & Goldberg, M. E. (1992). The updating of the representation of visual space in parietal cortex by intended eye movements. *Science*, *255*(5040), 90–92. <http://dx.doi.org/10.1126/science.1553535>.
- Edelman, J. A., & Goldberg, M. E. (2002). Effect of short-term saccadic adaptation on saccades evoked by electrical stimulation in the primate superior colliculus. *Journal of Neurophysiology*, *87*(4), 1915–1923.
- Fitzgibbon, E. J., & Goldberg, M. E. (1986). Cellular activity in the monkey superior colliculus during short term saccadic adaptation. *Society for Neuroscience*, *325*, 12. Abstr..
- Frens, M. A., & Van Opstal, A. J. (1997). Monkey superior colliculus activity during short-term saccadic adaptation. *Brain Research Bulletin*, *43*(5), 473–483.
- Fujita, M., Amagai, A., Minakawa, F., & Aoki, M. (2002). Selective and delay adaptation of human saccades. *Cognitive Brain Research*, *13*(1), 41–52.
- Goldberg, M. E., Musil, S. Y., Fitzgibbon, E. J., Smith, M. K., & Olson, C. R. (1993). The role of the cerebellum in the control of saccadic eye movements. In N. Mano (Ed.), *Cerebellum and basal ganglia in the control of movement* (pp. 203–211). Amsterdam: Elsevier.
- Golla, H., Tziridis, K., Haarmeier, T., Catz, N., Barash, S., & Thier, P. (2008). Reduced saccadic resilience and impaired saccadic adaptation due to cerebellar disease. *European Journal of Neuroscience*, *27*(1), 132–144.
- Guthrie, B. L., Porter, J. D., & Sparks, D. L. (1983). Corollary discharge provides accurate eye position information to the oculomotor system. *Science*, *221*(4616), 1193–1195. <http://dx.doi.org/10.1126/science.6612334>.
- Hallett, P. E., & Lightstone, A. D. (1976). Saccadic eye movements towards stimuli triggered by prior saccades. *Vision Research*, *16*(1), 99–106. [http://dx.doi.org/10.1016/0042-6989\(76\)90083-3](http://dx.doi.org/10.1016/0042-6989(76)90083-3).
- Herman, J. P., Blangero, A., Madelain, L., Khan, A., & Harwood, M. R. (2013). Saccade adaptation as a model of flexible and general motor learning. *Experimental Eye Research*, *114*, 6–15. <http://dx.doi.org/10.1016/j.exer.2013.04.001>.
- Herman, J. P., Harwood, M. R., & Wallman, J. (2009). Saccade adaptation specific to visual context. *Journal of Neurophysiology*, *101*(4), 1713–1721.
- Hopp, J. J., & Fuchs, A. F. (2002). Investigating the site of human saccadic adaptation with express and targeting saccades. *Experimental Brain Research*, *144*(4), 538–548.
- Hopp, J. J., & Fuchs, A. F. (2004). The characteristics and neuronal substrate of saccadic eye movement plasticity. *Progress in Neurobiology*, *72*(1), 27–53. <http://dx.doi.org/10.1016/j.pneurobio.2003.12.002>.
- Hopp, J. J., & Fuchs, A. F. (2010). Identifying sites of saccade amplitude plasticity in humans: transfer of adaptation between different types of saccade. *Experimental Brain Research*, *202*(1), 129–145.
- Iwamoto, Y., & Kaku, Y. (2010). Saccade adaptation as a model of learning in voluntary movements. *Experimental Brain Research*, *204*(2), 145–162. <http://dx.doi.org/10.1007/s00221-010-2314-3>.
- Joiner, W. M., FitzGibbon, E. J., & Wurtz, R. H. (2010). Amplitudes and directions of individual saccades can be adjusted by corollary discharge. *Journal of Vision*, *10*(2), 22. <http://dx.doi.org/10.1167/10.2.22>.
- Kojima, Y., Fuchs, A. F., & Soetedjo, R. (2015). Adaptation and adaptation transfer characteristics of five different saccade types in the monkey. *Journal of Neurophysiology*, *114*(1), 125–137.
- Li, C. S. R., & Andersen, R. A. (2001). Inactivation of macaque lateral intraparietal area delays initiation of the second saccade predominantly from contralesional eye positions in a double-saccade task. *Experimental Brain Research*, *137*(1), 45–57. <http://dx.doi.org/10.1007/s002210000546>.
- McLaughlin, S. C. (1967). Parametric adjustment in saccadic eye movements. *Perception & Psychophysics*, *2*(8), 359–362. <http://dx.doi.org/10.3758/BF03210071>.
- Medendorp, W. P., Goltz, H. C., Vilis, T., & Crawford, J. D. (2003). Gaze-centered updating of visual space in human parietal cortex. *The Journal of Neuroscience*, *23*(15), 6209–6214.
- Noto, C., Watanabe, S., & Fuchs, A. (1999). Characteristics of simian adaptation fields produced by behavioral changes in saccadic gain and direction. *Journal of Neurophysiology*, *81*, 2798–2813.
- Panouillères, M., Habchi, O., Gerardin, P., Salemme, R., Urquizar, C., Farne, A., & Pélisson, D. (2012). A role for the parietal cortex in sensorimotor adaptation of saccades. *Cerebral Cortex*.
- Pélisson, D., Alahyane, N., Panouillères, M., & Tilikete, C. (2010). Sensorimotor adaptation of saccadic eye movements. *Neuroscience & Biobehavioral Reviews*, *34*(8), 1103–1120.
- Provis, J. M., Dubis, A. M., Maddess, T., & Carroll, J. (2013). Adaptation of the central retina for high acuity vision: cones, the fovea and the avascular zone. *Progress in Retinal and Eye Research*, *35*, 63–81. <http://dx.doi.org/10.1016/j.preteyeres.2013.01.005>.
- Quessy, S., Quinet, J., & Freedman, E. G. (2010). The locus of motor activity in the superior colliculus of the rhesus monkey is unaltered during saccadic adaptation. *The Journal of Neuroscience*, *30*(42), 14235–14244.
- Rolfs, M., Knapen, T., & Cavanagh, P. (2010). Global saccadic adaptation. *Vision Research*, *50*(18), 1882–1890. <http://dx.doi.org/10.1016/j.visres.2010.06.010>.
- Soetedjo, R., & Fuchs, A. F. (2006). Complex spike activity of purkinje cells in the oculomotor vermis during behavioral adaptation of monkey saccades. *Journal of Neuroscience*, *26*, 7741–7755.
- Sommer, M. A., & Wurtz, R. H. (2002). A pathway in primate brain for internal monitoring of movements. *Science*, *296*(5572), 1480–1482.
- Sommer, M. A., & Wurtz, R. H. (2004). What the brain stem tells the frontal cortex. II. Role of the SC-MD-FEF pathway in corollary discharge. *Journal of Neurophysiology*, *91*(3), 1403–1423.
- Sommer, M. A., & Wurtz, R. H. (2006). Influence of the thalamus on spatial visual processing in frontal cortex. *Nature*, *444*(7117), 374–377. <http://dx.doi.org/10.1038/nature05279>.

- Takagi, M., Zee, D. S., & Tamargo, R. J. (1998). Effects of lesions of the oculomotor vermis on eye movements in primate: Saccades. *Journal of Neurophysiology*, *80*, 1911–1931.
- Takeichi, N., Kaneko, C. R., & Fuchs, A. F. (2007). Activity changes in monkey superior colliculus during saccade adaptation. *Journal of Neurophysiology*, *97*(6), 4096–4107.
- Tanaka, M. (2003). Contribution of signals downstream from adaptation to saccade programming. *Journal of Neurophysiology*, *90*(3), 2080–2086. <http://dx.doi.org/10.1152/jn.00207.2003>.
- Zimmermann, E. (2013). The reference frames in saccade adaptation. *Journal of Neurophysiology*, *109*(7), 1815–1823.